MIKAILALSYS
Journal of Multidisciplinary Sciences

e-ISSN : 2987-2286
p-ISSN : 2987-3924

Index: Harvard, Boston, Sydney, Copernicus, Sinta 4, Scilit, Semantic, Google, etc

https://doi.org/10.58578/mikailalsys.v4i3.11560

Effect of Bioreductant–Precursor Ratio on the Physical Characteristics of Silver Nanoparticles Synthesized via Green Synthesis Using Lemongrass (*Cymbopogon citratus*) and Betel Leaf (*Piper betle* L.) Extracts

Andini Khairi Alena, Riri Jonuarti, Leni Aziyus Fitri, Eka Susanti
Universitas Negeri Padang, Indonesia
andinikhairialena@gmail.com

Article Info:

Submitted:	Revised:	Accepted:	Published:
Jun 14, 2026	Jul 12, 2026	Jul 24, 2026	Jul 29, 2026

Abstract

Green synthesis of silver nanoparticles (AgNPs) using plant extracts offers an environmentally sustainable alternative to conventional synthesis methods; however, the influence of the bioreductant-to-precursor ratio in dual-bioreductant systems on the physical characteristics of AgNPs remains insufficiently understood. This study aimed to determine the effect of different bioreductant-to-precursor ratios on the physical characteristics of AgNPs synthesized using combined lemongrass (*Cymbopogon citratus*) and betel leaf (*Piper betle* L.) extracts. AgNPs were synthesized at bioreductant-to-precursor ratios of 1:9, 2:8, and 3:7 and characterized using UV–Visible spectroscopy, X-ray diffraction (XRD), and particle size analysis (PSA). UV–Visible spectroscopy confirmed the formation of AgNPs through the appearance of surface plasmon resonance peaks across all ratio variations. The 1:9 ratio exhibited the strongest optical characteristics, with a maximum absorption wavelength of 423 nm and the highest absorbance value of 2.165. XRD analysis verified the formation of AgNPs with a face-centered cubic crystalline structure and average crystallite

Mikailalsys is licensed under a Creative Commons Attribution-NonCommercial-ShareAlike 4.0 International License

sizes ranging from 18.45 to 23.80 nm. PSA results showed hydrodynamic particle diameters ranging from 38.3 to 137.7 nm and polydispersity index values of 0.096–0.306. An integrated evaluation of the characterization results identified the 1:9 ratio as the optimum synthesis condition because it produced the best balance between smaller particle size and higher surface plasmon resonance intensity. Nevertheless, the 2:8 ratio yielded the most homogeneous particle size distribution, as indicated by the lowest polydispersity index. These findings demonstrate that the bioreductant-to-precursor ratio critically influences the optical, structural, and particle-size characteristics of AgNPs. This study contributes to the optimization of environmentally sustainable AgNP synthesis using complementary plant-derived bioreductants.

Keywords: Bioreductant-to-Precursor Ratio; Dual Bioreductant; Green Synthesis; Particle Size Distribution; Silver Nanoparticles

INTRODUCTION

Silver nanoparticles (AgNPs) are among the most extensively studied nanostructured materials because their physical characteristics play a critical role in determining their performance across a wide range of applications. These characteristics include particle size, size distribution, morphology, crystallinity, and colloidal stability, all of which influence the optical, electronic, catalytic, and surface reactivity properties of AgNPs compared with bulk silver materials (Eker et al., 2025; Fahim et al., 2024; Kaabipour & Hemmati, 2021; Vanlalveni et al., 2021). Owing to these unique properties, AgNPs have been widely applied in various fields, including optical sensors, catalysts, electronic devices, environmental remediation, drug delivery systems, and antimicrobial materials. Therefore, controlling the physical characteristics during the synthesis process is essential, as even minor variations in synthesis conditions can lead to significant changes in material properties, ultimately affecting the performance of AgNPs in their intended applications (Dhir et al., 2024; Fahim et al., 2024; Kaabipour & Hemmati, 2021; Madhusudanan et al., 2025).

One of the rapidly developing approaches for producing AgNPs is green synthesis, which utilizes natural biomolecules as both reducing and stabilizing agents, making it a more environmentally friendly alternative to conventional chemical synthesis methods (Abada et al., 2024; Kaabipour & Hemmati, 2021; Vanlalveni et al., 2021). Various plant secondary metabolites, such as flavonoids, phenolic compounds, terpenoids, alkaloids, and saponins, are capable of donating electrons to reduce Ag^{+} ions into Ag^{0} while simultaneously forming

a capping layer that enhances nanoparticle stability (Dhir et al., 2024; Fahim et al., 2024; Huston et al., 2021). The success of green synthesis depends not only on the type of bioreductant employed but also on several synthesis parameters, including precursor concentration, pH, temperature, reaction time, and the bioreductant-to-precursor ratio. These parameters regulate the kinetics of Ag^+ ion reduction, nucleation, crystal growth, and nanoparticle aggregation, thereby determining the particle size, morphology, crystallinity, and stability of the resulting AgNPs (Abada et al., 2024; Eker et al., 2025; Kurra et al., 2025; Shafiq et al., 2023).

Among the various synthesis parameters, the bioreductant-to-precursor ratio is one of the most critical because it governs the balance between the amount of reducing biomolecules and the availability of Ag^+ ions throughout the synthesis (Kurra et al., 2025; Shafiq et al., 2023). Variations in this ratio influence the nucleation rate, crystal growth, and the effectiveness of nanoparticle stabilization, consequently affecting the particle size, size distribution, morphology, and crystallinity of the synthesized AgNPs AgNPs (Eker et al., 2025; Fahim et al., 2024; Shafiq et al., 2023). Therefore, the influence of the bioreductant-to-precursor ratio should be evaluated using characterization techniques capable of comprehensively describing the physical characteristics of nanoparticles. These characteristics are commonly analyzed using UV–Visible spectroscopy, X-ray diffraction (XRD), and a Particle Size Analyzer (PSA), as these techniques complement one another in evaluating the optical properties, crystal structure, crystallite size, hydrodynamic diameter, and particle size distribution of AgNPs (Dawadi et al., 2021; Fahim et al., 2024).

Various plant extracts have been employed as bioreductants in the green synthesis of AgNPs because they contain secondary metabolites capable of reducing metal ions while simultaneously stabilizing the resulting nanoparticles. One of the most widely utilized plants is lemongrass (*Cymbopogon citratus*), which contains flavonoids, phenolic acids, tannins, terpenoids, and citral that function as both reducing and stabilizing agents during nanoparticle nanopartikel (Du et al., 2024). By (Kurra et al., 2025) reported that variations in synthesis conditions using lemongrass extract affected the surface plasmon resonance (SPR) peak position, hydrodynamic diameter, polydispersity index (PDI), and stability of AgNPs, whereas (Cherian et al., 2025) obtained predominantly spherical AgNPs with particle sizes ranging from approximately 13.1 to 30.9 nm. These findings indicate that the phytochemical composition of lemongrass plays a significant role in controlling the reduction process,

nucleation, crystal growth, and nanoparticle stabilization, thereby influencing the physical characteristics of the synthesized AgNPs (Eker et al., 2025; Fahim et al., 2024; Kaabipour & Hemmati, 2021).

In addition to lemongrass, betel leaf (*Piper betle* L.) also has considerable potential as a bioreductant for the green synthesis of AgNPs because it is rich in phenolic compounds, flavonoids, tannins, alkaloids, hydroxychavicol, eugenol, and chavicol, all of which exhibit strong antioxidant activity (Singh et al., 2025). These phytochemicals act as electron donors to reduce Ag^{+} ions into Ag^{0} while simultaneously forming a capping layer that enhances nanoparticle stability (Dhir et al., 2024; Fahim et al., 2024). By (Tran et al., 2025) reported that betel leaf extract produced predominantly spherical AgNPs with an average particle size of approximately 20 nm and a face-centered cubic (fcc) crystal structure. The differences in the phytochemical compositions of lemongrass and betel leaf suggest that these two extracts may provide complementary reduction and stabilization mechanisms. Consequently, their combination is expected to produce AgNPs with physical characteristics distinct from those synthesized using a single plant extract.

Numerous studies have demonstrated that plant extracts are effective bioreductants for the green synthesis of AgNPs. However, most previous studies have employed single plant extracts and primarily focused on optimizing extract concentration, precursor concentration, pH, temperature, and reaction time to obtain smaller particle sizes or enhanced biological activity (Kurra et al., 2025; Shafiq et al., 2023; Vanlalveni et al., 2021). Based on the recent literature, studies investigating the use of combined plant extracts as a dual-bioreductant system, particularly to evaluate the effect of the bioreductant-to-precursor ratio on the physical characteristics of AgNPs, remain very limited (Abada et al., 2024; Eker et al., 2025; Fahim et al., 2024; Madhusudanan et al., 2025). Therefore, further investigation into the relationship between the bioreductant-to-precursor ratio, nanoparticle formation mechanisms, and the physical characteristics of AgNPs is necessary to provide a scientific basis for developing more rational and efficient green synthesis strategies.

The physical characteristics of AgNPs were evaluated using UV–Visible spectroscopy, X-ray diffraction (XRD), and a Particle Size Analyzer (PSA) to determine their optical properties, crystal structure, crystallite size, hydrodynamic diameter, and particle size distribution. The novelty of this study lies in the use of a combination of lemongrass and betel leaf extracts as a dual-bioreductant system, the investigation of the influence of the

bioreductant-to-precursor ratio on the mechanism of AgNP formation, and the integrated evaluation of nanoparticle physical characteristics using UV–Visible spectroscopy, XRD, and PSA. The findings of this study are expected to provide a scientific foundation for developing more rational, efficient, and sustainable strategies for optimizing the green synthesis of AgNPs to produce nanoparticles with well-controlled physical characteristics tailored to specific applications. Accordingly, this study was conducted to analyze the effect of the bioreductant-to-precursor ratio on the physical characteristics of AgNPs synthesized via green synthesis using a combination of lemongrass (*Cymbopogon citratus*) and betel leaf (*Piper betle* L.) extracts.

METHODS

Fresh lemongrass (*Cymbopogon citratus*) and betel leaf (*Piper betle* L.) cultivated locally in Air Tawar Barat were collected in February 2026 and used as bioreductant sources for the synthesis of silver nanoparticles. Silver nitrate ($AgNO_3$; Chemical Pure, 99.54% purity) was obtained from PT ROFA Laboratorium Indonesia, while 70% ethanol and distilled water were supplied by PT Novalindo Jaya Utama. All chemicals were used without further purification.

The lemongrass (*Cymbopogon citratus*) and betel leaf (*Piper betle* L.) samples were washed under running water, rinsed with distilled water, air-dried at room temperature (±27 °C) for 24 h, and subsequently oven-dried at 50 °C until a constant weight was achieved. The dried samples were ground into fine powder using a grinder. A total of 100 g of each powdered leaf sample was extracted with 1000 mL of 70% ethanol using the Ultrasonic-Assisted Extraction (UAE) method at 35 °C for 15 min, and the extraction was repeated three times. The filtrates from the three extraction cycles were combined separately for each plant species and concentrated using a rotary evaporator at 60 °C until a concentrated extract was obtained. The concentrated extracts were then reconstituted with distilled water to a final concentration of 5% (w/v).

A 1 mM $AgNO_3$ solution was prepared by dissolving 0.1699 g of $AgNO_3$ in distilled water and adjusting the final volume to 1000 mL. The lemongrass and betel leaf extracts were mixed at a volume ratio of 1:1 (v/v) and subsequently reacted with the $AgNO_3$ solution at bioreductant-to-precursor volume ratios of 1:9, 2:8, and 3:7, with a total reaction volume of

300 mL for each treatment. The reaction mixtures were homogenized using a magnetic stirrer for 5 min and then incubated at room temperature for 60 min under light-protected conditions. The formation of AgNPs was indicated by a color change from a clear solution to yellowish-brown and finally dark brown. The suspensions were subsequently allowed to stand at room temperature for 24 h to facilitate nanoparticle growth and stabilization.

The AgNP suspensions were centrifuged at 10,000 rpm for 20 min. The resulting precipitates were washed three times with distilled water through repeated resuspension and centrifugation to remove residual organic compounds and unreacted Ag^+ ions. The purified precipitates were then dried in an oven at 50 °C until a constant weight was obtained.

The optical properties of the AgNPs were characterized using UV–Visible spectroscopy over a wavelength range of 300–700 nm to confirm nanoparticle formation through the characteristic surface plasmon resonance (SPR) absorption peak, which typically appears between 420 and 450 nm (Tran et al., 2025), and to evaluate the effect of the bioreductant-to-precursor ratio on the position and intensity of the SPR peak. A red shift of λmax toward longer wavelengths indicates an increase in particle size (Tran et al., 2025), whereas a narrower and sharper SPR peak suggests a more homogeneous particle size distribution (Cherian et al., 2025). The spectral data were analyzed using Origin software.

The crystal structure of the AgNPs was characterized using X-ray diffraction (XRD) over a 2θ range of 20°–80° to identify the metallic silver (Ag^0) phase and confirm the face-centered cubic (fcc) crystal structure through the characteristic diffraction peaks at 2θ values of 38°, 44°, 64°, and 77°, corresponding to the (111), (200), (220), and (311) crystallographic planes according to JCPDS No. 03-0921 (Cherian et al., 2025). XRD analysis was also performed to evaluate the influence of the bioreductant-to-precursor ratio on crystallinity and crystallite size. The diffraction data were analyzed using Origin software, and the average crystallite size was calculated using the Debye–Scherrer equation:

$$D = \frac{k\lambda}{\beta cos\theta}$$

where D is the average crystallite size (nm), k is the shape factor (commonly taken as 0.94), λ is the X-ray wavelength, β is the full width at half maximum (FWHM) expressed in radians, and θ is the Bragg angle.

Particle size and size distribution were characterized using a Particle Size Analyzer (PSA) based on Dynamic Light Scattering (DLS) to determine the average hydrodynamic

diameter and the polydispersity index (PDI) based on fluctuations in light scattering caused by the Brownian motion of particles (Kurra et al., 2025). A low PDI value indicates a monodisperse particle population, whereas a higher PDI value reflects greater size heterogeneity (Kurra et al., 2025). The data were analyzed using the instrument's proprietary software.

RESULTS

1. Optical Characteristics of Silver Nanoparticles (UV–Visible Spectroscopy)

The formation of AgNPs at all bioreductant-to-precursor ratios was confirmed by the appearance of a characteristic surface plasmon resonance (SPR) peak in the UV–Visible spectra (Figure 1). The obtained λmax values were 423 nm (1:9), 445 nm (2:8), and 394 nm (3:7), with corresponding absorbance values of 2.165, 2.017, and 1.692, respectively (Table 1). The differences in the SPR peak position and intensity indicate that variations in the bioreductant-to-precursor ratio influenced the optical characteristics of the synthesized AgNPs.

Table 1. Maximum wavelength (λmax) and SPR peak absorbance of AgNPs at different bioreductant-to-precursor ratios.

Bioreductant:Precursor Ratio	Wavelength (nm)	Absorbance
1:9	423	2.165
2:8	445	2.017
3:7	394	1.692

The UV–Visible spectra shown in Figure 1 demonstrate that each ratio produced a distinct SPR peak position and intensity. The SPR peak of the 1:9 ratio appeared at 423 nm with the highest absorbance intensity, whereas the 2:8 ratio exhibited a shift toward a longer wavelength (red shift) to 445 nm. In contrast, the 3:7 ratio displayed a shift toward a shorter wavelength (blue shift) to 394 nm, accompanied by a decrease in absorbance intensity.

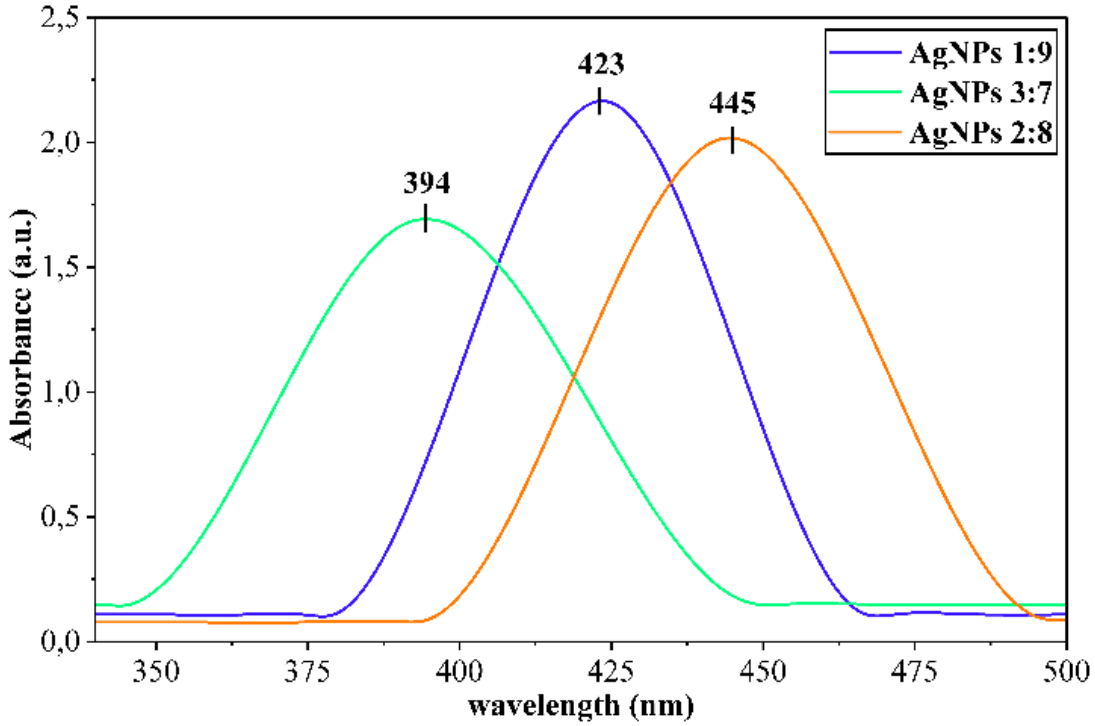


Figure 1. UV–Visible spectra of silver nanoparticles (AgNPs) synthesized via green synthesis using a combination of lemongrass and betel leaf extracts at bioreductant-to-precursor ratios of 1:9, 2:8, and 3:7.

2. Crystal Structure Characteristics (X-Ray Diffraction)

The X-ray diffraction (XRD) patterns of the green-synthesized AgNPs prepared at different bioreductant-to-precursor ratios are presented in Figure 2. All samples exhibited four major diffraction peaks at 2θ values of approximately 38°, 44°, 64°, and 77°, corresponding to the (111), (200), (220), and (311) crystal planes, respectively. These characteristic peaks confirm the formation of the face-centered cubic (fcc) crystal structure typical of silver nanoparticles.

The crystallite size calculated using the Debye–Scherrer equation yielded average crystallite sizes of 19.04 nm for the 1:9 ratio, 23.80 nm for the 2:8 ratio, and 18.45 nm for the 3:7 ratio (Table 2).

Table 2. 2θ position, Miller index (hkl), FWHM, and crystallite size of AgNPs determined by XRD analysis at different bioreductant-to-precursor ratios.

Ratio	2θ (°)	Hkl	FWHM	Crystallite Size (nm)
1:9	38.11	(111)	0.38462	21.85
	44.30	(200)	0.43258	19.83
	64.48	(220)	0.44684	21.03

Ratio	2θ (°)	Hkl	FWHM	Crystallite Size (nm)
	77.42	(311)	0.75673	13.46
2:8	38.15	(111)	0.42969	19.57
	44.26	(200)	0.32987	26.00
	64.42	(220)	0.40074	23.40
	77.45	(311)	0.38832	26.22
3:7	38.18	(111)	0.40535	20.75
	44.36	(200)	0.58660	14.65
	64.55	(220)	0.45237	20.79
	77.45	(311)	0.57796	17.61

The diffraction patterns indicate that for the 1:9 and 2:8 ratios, the diffraction peak corresponding to the (111) crystal plane exhibited the highest intensity compared with the other crystallographic planes. In contrast, the 3:7 ratio showed an increased intensity of the (200) diffraction peak together with the appearance of additional diffraction peaks outside the characteristic AgNP reflections.

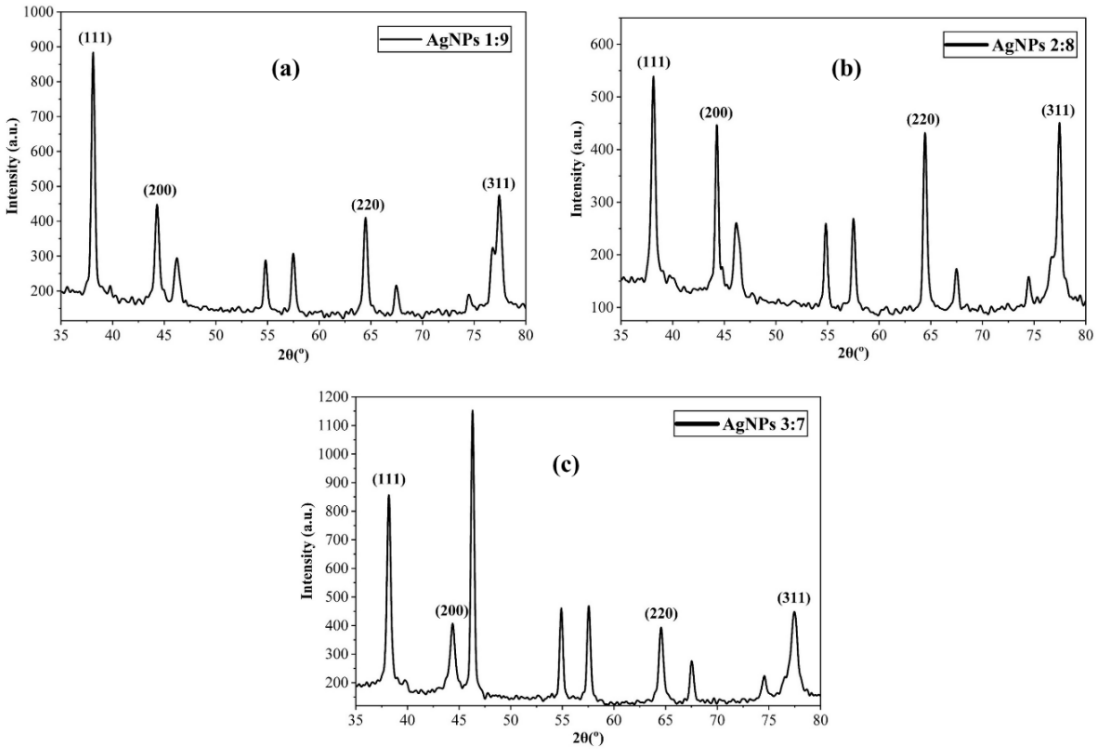


Figure 2. X-ray diffraction (XRD) patterns of AgNPs synthesized at bioreductant-to-precursor ratios of (a) 1:9, (b) 2:8, and (c) 3:7.

3. Particle Size Characteristics (Particle Size Analyzer)

The Particle Size Analyzer (PSA) results demonstrated that variations in the bioreductant-to-precursor ratio affected both the hydrodynamic diameter and the particle size distribution of the synthesized AgNPs (Table 3). The average hydrodynamic diameters obtained were 38.3 nm (1:9), 137.7 nm (2:8), and 53.7 nm (3:7), with corresponding polydispersity index (PDI) values of 0.306, 0.096, and 0.269, respectively. The particle size distribution curves shown in Figure 3 indicate that each ratio produced a distinct distribution profile.

Table 3. Average hydrodynamic diameter and polydispersity index (PDI) of AgNPs determined by PSA analysis at different bioreductant-to-precursor ratios.

Bioreductant:Precursor Ratio	Hydrodynamic Diameter (nm)	PDI
1:9	38.3	0.306
2:8	137.7	0.096
3:7	53.7	0.269

The particle size intensity distribution curves presented in Figure 3 demonstrate that each ratio produced a different distribution pattern. These differences indicate variations in both the hydrodynamic particle size and the degree of particle homogeneity under each synthesis condition.

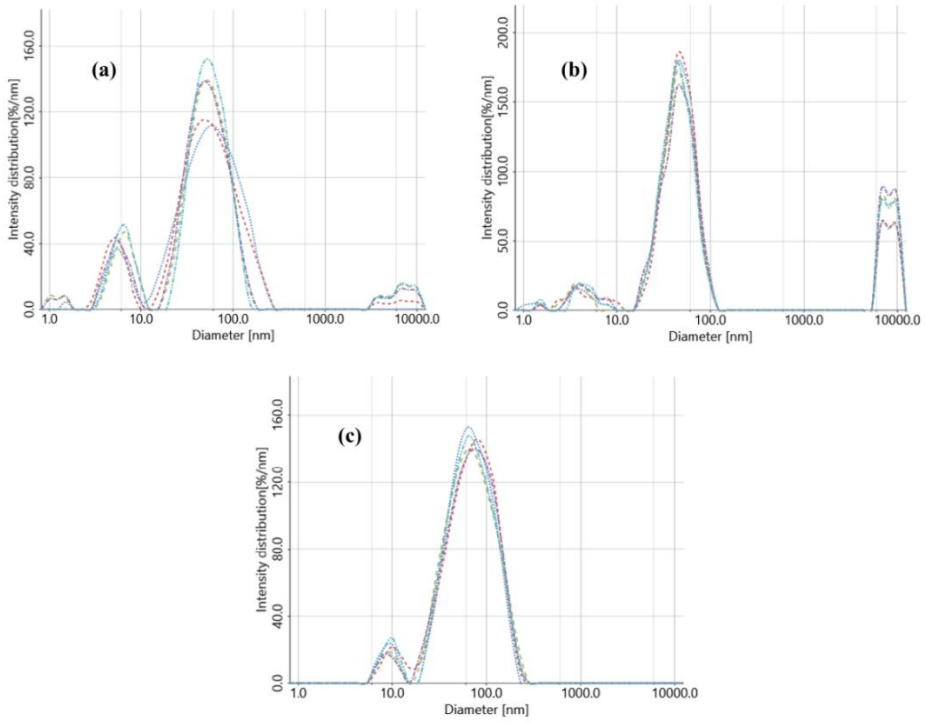


Figure 3. Intensity size distribution curves of AgNPs obtained from Particle Size Analyzer (PSA) measurements at bioreductant-to-precursor ratios of (a) 1:9, (b) 2:8, and (c) 3:7.

Figure 3 further shows that the intensity size distribution of AgNPs differed among the bioreductant-to-precursor ratios. The 1:9 ratio produced a distribution with a smaller hydrodynamic particle size, whereas the 2:8 ratio exhibited a narrower distribution peak, indicating a more homogeneous particle size distribution. In contrast, the 3:7 ratio displayed a broader distribution, suggesting a higher degree of particle size heterogeneity. These differences in distribution patterns demonstrate that the bioreductant-to-precursor ratio significantly influences the hydrodynamic size and particle uniformity of the synthesized AgNPs.

DISCUSSION

1. Optical Characteristics of Silver Nanoparticles (UV–Visible Spectroscopy)

The differences in the position and intensity of the surface plasmon resonance (SPR) bands indicate that variations in the bioreductant-to-precursor ratio influence the formation process of AgNPs. The SPR peaks observed within the range of 394–445 nm confirm the formation of silver nanoparticles and remain within the characteristic range of spherical AgNPs reported in various studies (Fahim et al., 2024).

The 1:9 ratio produced an SPR peak at 423 nm with the highest absorbance intensity. This condition indicates that the reduction process of Ag^{+} ions occurred more effectively, resulting in a higher concentration of AgNPs. In addition, the relatively sharp SPR peak suggests a more uniform particle size distribution with a lower degree of aggregation (Cherian et al., 2025).

At the 2:8 ratio, a red shift occurred toward 445 nm accompanied by a decrease in absorbance intensity. This phenomenon indicates a tendency toward increased particle size or enhanced interparticle interactions due to the dominance of crystal growth processes over nucleation processes (Fahim et al., 2024). Conversely, the 3:7 ratio exhibited a blue shift to 394 nm, accompanied by decreased absorbance intensity and broadening of the SPR band. This condition suggests that an excessive amount of bioreductant accelerated the reduction process, causing nanoparticle formation and stabilization to become less controlled and resulting in a more heterogeneous particle size distribution (Shafiq et al., 2023).

Overall, the UV–Visible analysis demonstrates that the bioreductant-to-precursor ratio influences the optical characteristics of AgNPs through changes in SPR position,

absorbance intensity, and spectral profile. These findings were further confirmed through crystal structure analysis using XRD and particle size characterization using PSA to provide a more comprehensive understanding of the physical characteristics of AgNPs.

2. Crystal Structure Characteristics (X-Ray Diffraction)

XRD characterization confirmed that all variations of the bioreductant-to-precursor ratio successfully produced AgNPs with a face-centered cubic (fcc) crystal structure, as indicated by the appearance of four diffraction peaks corresponding to the (111), (200), (220), and (311) crystal planes, in agreement with the standard diffraction pattern of metallic silver (JCPDS No. 03-0921). These results are consistent with previous studies reporting that the fcc structure represents the typical crystalline phase of green-synthesized AgNPs (Vanlalveni et al., 2021; Fahim et al., 2024).

For the 1:9 and 2:8 ratios, the diffraction peak corresponding to the (111) plane exhibited the highest intensity, indicating dominant crystal growth along the plane with the lowest surface energy, which reflects good crystallinity (Fahim et al., 2024). In contrast, the 3:7 ratio exhibited additional diffraction peaks beyond the characteristic Ag reflections, suggesting the possible presence of minor phases or residual phytochemical compounds due to the increased proportion of bioreductant, although the crystalline Ag phase was still successfully formed.

The average crystallite size was influenced by the bioreductant-to-precursor ratio, with the largest value obtained for the 2:8 ratio (23.80 nm), followed by the 1:9 ratio (19.04 nm) and the 3:7 ratio (18.45 nm). This finding indicates that the 2:8 ratio promoted crystal growth more effectively than nucleation, resulting in larger crystalline domains (Shafiq et al., 2023). However, crystallite size only represents the size of crystalline domains and does not necessarily correspond directly to particle size or nanoparticle aggregation level.

Overall, the XRD results demonstrate that variations in the bioreductant-to-precursor ratio affect the crystal growth process without altering the fundamental crystal structure of AgNPs, which remains face-centered cubic. Therefore, these findings require further confirmation through PSA analysis to evaluate the relationship between crystallite size, hydrodynamic diameter, and particle size distribution more comprehensively.

3. Particle Size Characteristics (Particle Size Analyzer)

Variations in the bioreductant-to-precursor ratio affected the hydrodynamic diameter and homogeneity of AgNPs. The 1:9 ratio produced the smallest hydrodynamic diameter (38.3 nm), whereas the 2:8 ratio produced the largest diameter (137.7 nm) with the lowest polydispersity index (PDI) value (0.096), indicating the most homogeneous particle size distribution. Meanwhile, the 3:7 ratio resulted in a hydrodynamic diameter of 53.7 nm with a PDI value of 0.269, indicating a more heterogeneous particle size distribution. These differences demonstrate that changes in the bioreductant-to-precursor ratio influence the formation, growth, and stabilization processes of AgNPs during synthesis (Shafiq et al., 2023).

The 1:9 ratio produced the smallest hydrodynamic size and was consistent with the UV–Visible results, which showed the sharpest SPR peak with the highest absorbance intensity, indicating more effective AgNP formation. In contrast, the 2:8 ratio exhibited the largest hydrodynamic diameter and crystallite size based on XRD analysis but showed the lowest PDI value, indicating the most homogeneous particle size distribution. For the 3:7 ratio, although the hydrodynamic size was smaller than that of the 2:8 ratio, the decrease in absorbance intensity observed in the UV–Visible spectrum and the appearance of additional diffraction peaks in the XRD pattern suggest that an excessive amount of bioreductant caused the synthesis process to become less controlled.

The determination of the optimum ratio in this study prioritized particle size and SPR intensity as the main indicators because both parameters are directly related to the specific surface area and reactivity of AgNPs, which determine their application performance. Meanwhile, PDI was used as a supporting parameter to evaluate particle population uniformity. The PDI value of the 1:9 ratio (0.306) was indeed higher than that of the 2:8 ratio (0.096); however, this value remains within the range of relatively narrow to moderate size distribution for dynamic light scattering-based measurements, considering that particle populations are generally categorized as highly polydisperse when the PDI approaches or exceeds 0.7 (Danaei et al., 2018). Therefore, the PDI value of the 1:9 ratio does not indicate significant heterogeneity or aggregation.

Overall, the integrated evaluation of UV–Visible, XRD, and PSA results demonstrates that the 1:9 ratio provides the best balance between optical characteristics, particle size, and crystal structure, making it the most optimum AgNP synthesis condition

among the three tested ratios. This determination should be further confirmed through functional property evaluations of AgNPs, such as antibacterial or catalytic activity assessments, to verify whether the observed advantages in physical characteristics are also reflected in their application performance.

CONCLUSION

This study demonstrates that variations in the bioreductant ratio significantly influence the physical characteristics of silver nanoparticles (AgNPs) synthesized through a green synthesis approach using a combination of lemongrass (*Cymbopogon citratus*) and betel leaf (*Piper betle* L.) extracts. The results of UV–Visible spectroscopy, X-ray diffraction (XRD), and Particle Size Analyzer (PSA) analyses indicate that each ratio produces distinct characteristics; therefore, the determination of the optimum synthesis condition cannot be based on a single characterization parameter. The 1:9 ratio exhibited the best optical characteristics, characterized by the sharpest surface plasmon resonance (SPR) peak and the highest absorbance intensity, while also producing the smallest hydrodynamic particle diameter. Meanwhile, the 2:8 ratio resulted in the largest crystallite size and the most homogeneous particle size distribution based on the lowest polydispersity index (PDI) value. Considering the integrated results of all characterization analyses, the 1:9 bioreductant ratio was determined as the optimum synthesis condition because it provided the best balance between optical properties, relatively small particle size, and favorable crystal structure. These findings indicate that optimization of green AgNP synthesis requires a multi-characterization approach to obtain nanoparticles with more controlled physical characteristics and potentially improved performance across various applications.

This study provides a scientific contribution to the development of green synthesis methods for silver nanoparticles by utilizing a combination of two natural bioreductants, namely lemongrass (*Cymbopogon citratus*) and betel leaf (*Piper betle* L.) extracts, which have been relatively rarely investigated simultaneously. In addition to demonstrating the effect of bioreductant ratio variations on the physical characteristics of AgNPs, this study offers a more comprehensive evaluation approach through the integration of UV–Visible spectroscopy, XRD, and PSA characterization results in determining the optimum synthesis condition. The findings of this study can serve as a scientific basis for developing more effective dual-bioreductant systems and provide references for future research in designing

plant-based nanoparticles with more stable, uniform, and application-oriented physical characteristics for various fields, including biomedical, environmental, and functional material applications.

Future studies are recommended to evaluate the functional properties of synthesized silver nanoparticles at each bioreductant ratio variation, including antibacterial, antioxidant, antifungal, photocatalytic activities, and cytotoxicity assessments, to confirm whether the 1:9 ratio also provides the best application performance. Furthermore, subsequent research may optimize other synthesis parameters, such as pH, reaction temperature, synthesis time, precursor concentration, and bioreductant extract concentration. Advanced characterization techniques, including SEM/TEM, FTIR, and zeta potential measurements, are also recommended to obtain more comprehensive information regarding nanoparticle morphology, stabilizing functional groups, and colloidal stability of AgNPs. Therefore, the development of green synthesis methods using a combination of lemongrass and betel leaf extracts is expected to produce silver nanoparticles with superior physical and functional characteristics, enabling their further development for broader-scale applications.

REFERENCES

Abada, E., Mashraqi, A., Modafer, Y., Al Abboud, M. A., & El-Shabasy, A. (2024). Review green synthesis of silver nanoparticles by using plant extracts and their antimicrobial activity. *Saudi Journal of Biological Sciences, 31*(1), 103877. https://doi.org/10.1016/j.sjbs.2023.103877

Dawadi, S., Katuwal, S., Gupta, A., Lamichhane, U., Thapa, R., Jaisi, S., Lamichhane, G., Bhattarai, D. P., & Parajuli, N. (2021). Current research on silver nanoparticles: Synthesis, characterization, and applications. *Journal of Nanomaterials, 2021*, 6687290. https://doi.org/10.1155/2021/6687290

Dhir, R., Chauhan, S., Subham, P., Kumar, S., Sharma, P., Shidiki, A., & Kumar, G. (2024). Plant-mediated synthesis of silver nanoparticles: Unlocking their pharmacological potential—A comprehensive review. *Frontiers in Bioengineering and Biotechnology, 11*, 1324805. https://doi.org/10.3389/fbioe.2023.1324805

Du, X., Zhang, M., Wang, S., Li, J., Zhang, J., & Liu, D. (2024). Ethnopharmacology, chemical composition and functions of *Cymbopogon citratus*. *Chinese Herbal Medicines, 16*(3), 358–374. https://doi.org/10.1016/j.chmed.2023.07.002

Eker, F., Akdaşçi, E., Duman, H., Bechelany, M., & Karav, S. (2025). Green synthesis of silver nanoparticles using plant extracts: A comprehensive review of physicochemical properties and multifunctional applications. *International Journal of Molecular Sciences, 26*(13), 6222. https://doi.org/10.3390/ijms26136222

Fahim, M., Shahzaib, A., Nishat, N., Jahan, A., Bhat, T. A., & Inam, A. (2024). Green synthesis of silver nanoparticles: A comprehensive review of methods, influencing

factors, and applications. *JCIS Open, 16*, 100125. https://doi.org/10.1016/j.jciso.2024.100125

Huston, M., DeBella, M., DiBella, M., & Gupta, A. (2021). Green synthesis of nanomaterials. *Nanomaterials, 11*(8), 2130. https://doi.org/10.3390/nano11082130

Kaabipour, S., & Hemmati, S. (2021). A review on the green and sustainable synthesis of silver nanoparticles and one-dimensional silver nanostructures. *Beilstein Journal of Nanotechnology, 12*, 102–136. https://doi.org/10.3762/bjnano.12.9

Kurra, H., Velidandi, A., Sarvepalli, M., Pabbathi, N. P. P., & Godishala, V. (2025). Aqueous *Cymbopogon citratus* extract mediated silver nanoparticles: Part I. Influence of synthesis parameters, characterization, and biomedical studies. *Nanomaterials, 15*(5), 328. https://doi.org/10.3390/nano15050328

Madhusudanan, M., Zhang, J., Pandit, S., Singh, P., Jeong, G.-J., Khan, F., & Mijakovic, I. (2025). Green synthesis of silver nanoparticles: A review of polymer and antimicrobial drug combinations for enhanced antimicrobial applications. *Advanced NanoBiomed Research, 5*(12), 2400194. https://doi.org/10.1002/anbr.202400194

Shafiq, A., Deshmukh, A. R., AbouAitah, K., & Kim, B.-S. (2023). Green synthesis of controlled shape silver nanostructures and their peroxidase, catalytic degradation, and antibacterial activity. *Journal of Functional Biomaterials, 14*(6), 325. https://doi.org/10.3390/jfb14060325

Singh, T., Shafi, Z., Singh, R., Bisht, B., Yadav, K. K., Algethami, J. S., Albakri, G. S., & Alreshidi, M. A. (2025). Microwave-assisted extraction of phytochemicals from *Piper betle* L.: Optimization, characterization, and bioactivity evaluation. *Food Chemistry: X, 29*, 102672. https://doi.org/10.1016/j.fochx.2025.102672

Sugiyono. (2023). *Metode Penelitian Pendidikan (Kuantitatif, Kualitatif, dan R&D)*. Alfabeta.

Vanlalveni, C., Lallianrawna, S., Biswas, A., Selvaraj, M., Changmai, B., & Rokhum, S. L. (2021). Green synthesis of silver nanoparticles using plant extracts and their antimicrobial activities: A review of recent literature. *RSC Advances, 11*(5), 2804–2837. https://doi.org/10.1039/D0RA09941D